Nuclear Physics A379 (1982) 313–329

EQUILIBRIUM TREATMENT OF SPIN-DEPOLARIZING MODES IN MASS ASYMMETRIC HEAVY-ION SYSTEMS

RICHARD P. SCHMITT

Department of Chemistry and Cyclotron Institute, Texas A & M University, College Station, Texas 77843, USA

and

ALBERTO J. PACHECO *

Nuclear Science Division, Lawrence Berkeley Laboratory, University of California, Berkeley, CA 94720, USA

Received 7 October 1981

Abstract: A two-sphere model is developed for the thermal excitation of spin-depolarizing modes in mass asymmetric heavy-ion systems. The effect of these modes on the spin distributions and the spin alignment of the fragments is investigated.

1. Introduction

Angular momentum transfer is currently a topic of considerable interest in the study of deep-inelastic processes. Because the l-transfer is linked to the incident l-wave, such studies provide insight into various dynamical features of heavy-ion collisions such as the strength of the frictional forces. An interesting aspect which has recently come to light concerns the alignment of the fragments spins. Experimental studies of γ-ray anisotropies and the angular distributions of sequential fission fragments and light particles have shown that the angular momenta of the fragments is not strictly perpendicular to the reaction plane, as suggested by simple friction models [1–7]). Instead, it appears that components of angular momentum are generated along other axes in the collision process. These angular momenta combine with the angular momentum transferred from the relative motion leading to a misalignment or depolarization of the fragment spins with respect to the normal to the reaction plane.

The existence of spin-depolarizing modes complicates the experimental determination of the angular momentum transfer in deep-inelastic reactions. For example, in sequential fission studies the excitation of these modes affect the out-of-plane and in-plane angular distributions of the fission fragments, which are used to extract the fragment spins. In the case of γ-ray multiplicity measurements, which are sensitive

* Permanent address: Comision Nacional de Energia Atomica, Buenos Aires, Argentina.

to the sum of the absolute values of the fragment spins, depolarizing modes can affect the magnitudes of the fragments' spins (especially for the low l-waves) as well as the higher moments of their spin distributions. Moreover, the partial loss of alignment makes it difficult to relate the multiplicity of continuum γ-rays to the angular momentum since the average multipolarity cannot be inferred from anisotropy data alone.

In the light of the above discussion, it is clear that a deeper understanding of spin-depolarizing effects is important to heavy-ion reaction studies. From a theoretical point of view, two approaches have been taken. The first of these involves the assumption of a particular mechanism (or mechanisms) such as particle transfer and/or the excitation of collective modes [8-10]). The second approach assumes the thermal excitation of a number of angular momentum bearing collective modes [11]). While this latter approach overlooks the very interesting dynamical aspects of the problem, it offers the advantage that it does not rely on the validity of a particular reaction mechanism, and, at the same time, provides the long-time limit to which all mechanisms must tend.

In a recent work, a macroscopic model has been developed which describes the thermal excitation of collective modes for a symmetric system consisting of two touching, rigid, liquid-drop spheres [11]). This model has proved useful in the interpretation of γ-ray anisotropies [5-7]). In the current work this model is extended to include asymmetric systems. This extention allows a much broader basis for comparison with experimental data.

2. Normal modes

For simplicity we shall assume that the dinuclear, intermediate complex consists of two rigid, liquid-drop spheres. In order to specify the locations and the orientations of these two objects in space, twelve coordinates are needed. By working in the center-of-mass system and by requiring that the fragments touch, six coordinates are effectively eliminated. Thus there are six normal modes of vibration (for spherical fragments the modes actually correspond to rotations).

If the system is mass symmetric, the normal modes can be determined essentially by inspection. They are bending (doubly degenerate), twisting, wriggling (doubly degenerate), and tilting [11]). The first three modes are antisymmetric (i.e. the angular momenta of the fragments are oppositely directed) while the last three are symmetric. In all cases the magnitude of the fragments' spins are equal. However, for asymmetric heavy-ion systems the normal coordinates are not readily apparent and must be determined by diagonalizing the kinetic energy matrix.

Let us treat the problem in a body-fixed coordinate system in which the disintegration axis is the y-axis (see fig. 1). The total angular momentum of the system, which is equal to the initial orbital angular momentum, is denoted by $\boldsymbol{I}$. The projection of $\boldsymbol{I}$

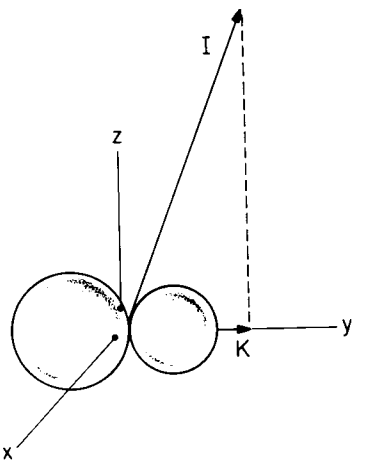

Fig. 1. Schematic of the dinuclear system in the body-fixed frame showing the total spin vector $\boldsymbol{I}$ and its projection on the symmetry axis K.

along the disintegration axis is K. In the body-fixed frame I precesses about the y-axis with an angular frequency Ω given by

$$\Omega = \left(\frac{\mathscr{I}_\perp - \mathscr{I}_{||}}{\mathscr{I}_\perp \mathscr{I}_{||}}\right) K,$$

where $\mathscr{I}_\perp$ and $\mathscr{I}_{||}$ are respectively the moments of inertia perpendicular and parallel to the symmetry axis. The components of $\boldsymbol{I}$ along the x- and z-axis are

$$I_x = \sqrt{I^2 - K^2}\,\sin \Omega t,$$

$$I_z = \sqrt{I^2 - K^2}\,\cos \Omega t.$$

When the complex decays, part of $\boldsymbol{I}$ will become intrinsic spin in the fragments and part will remain in the relative motion; that is,

$$\boldsymbol{I} = \boldsymbol{S}_1 + \boldsymbol{S}_2 + \boldsymbol{l}, \tag{1}$$

where $\boldsymbol{S}_1$ and $\boldsymbol{S}_2$ are the respective spins of the fragments and $\boldsymbol{l}$ is the final orbital angular momentum. The total rotational energy of the system is

$$E = \frac{l^2}{2\mathscr{I}_r} + \frac{S_1^2}{2\mathscr{I}_1} + \frac{S_2^2}{2\mathscr{I}_2}, \tag{2}$$

where $\mathscr{I}_r = \mu r^2$ is the relative moment of inertia and the quantities $\mathscr{I}_1$ and $\mathscr{I}_2$ are the moments of inertia of the two fragments.

The intrinsic spins of the fragments arise from two sources: the rigid rotation of the complex and the depolarizing modes. Thus the components of S_1 can be written as

$$S_{1x} = \frac{\mathscr{I}_1}{\mathscr{I}_T}\sqrt{I^2-K^2}\sin\Omega t + R_{1x} = I_{R1}\sin\Omega t + R_{1x}, \tag{3a}$$

$$S_{1y} = \frac{\mathscr{I}_1}{\mathscr{I}_1+\mathscr{I}_2}K + R_{1y}, \tag{3b}$$

$$S_{1z} = I_{R1}\cos\Omega t + R_{1z}, \tag{3c}$$

where $\mathscr{I}_T = \mathscr{I}_1 + \mathscr{I}_2 + \mathscr{I}_r$. In each of these equations the first term arises from rigid rotation and the second term is produced by the excitation of the collective modes. Obviously, similar equations hold for the spin components of fragment two.

Angular-momentum conservation imposes the following constraints:

$$I_x = \sqrt{I^2-K^2}\sin\Omega t = R_{1x}+R_{2x}+l_x+(I_{R1}+I_{R2})\sin\Omega t, \tag{4a}$$

$$I_y = K = R_{1y}+R_{2y}+\frac{\mathscr{I}_1}{\mathscr{I}_1+\mathscr{I}_2}K+\frac{\mathscr{I}_2}{\mathscr{I}_1+\mathscr{I}_2}K, \tag{4b}$$

$$I_z = \sqrt{I^2-K^2}\cos\Omega t = R_{1z}+R_{2z}+l_z+(I_{R1}+I_{R2})\cos\Omega t. \tag{4c}$$

As the second of these equations clearly shows, $R_{1y} = -R_{2y}$. Using eqs. (2), (3a-c) and (4a-c) it is straightforward to show that

$$\Delta E = E - \frac{I^2}{2\mathscr{I}_T} = \frac{R_{1x}^2+R_{1z}^2}{2\mathscr{I}_1}+\frac{R_{2x}^2+R_{2z}^2}{2\mathscr{I}_2}$$
$$+\frac{(R_{1x}+R_{2x})^2+(R_{1z}+R_{2z})^2}{2\mathscr{I}_r}+\frac{\mathscr{I}_r}{2(\mathscr{I}_1+\mathscr{I}_2)\mathscr{I}_T}K^2+\frac{\mathscr{I}_1+\mathscr{I}_2}{2\mathscr{I}_1\mathscr{I}_2}R_y^2, \tag{5}$$

where $R_y = R_{1y}$. The above quadratic form can be written as $\Delta E = \frac{1}{2}R^tTR$ where $R^t = (R_{1x}, R_{2x}, K, R_y, R_{1z}, R_{2z})$ and T is the kinetic energy tensor. Now T is block diagonal and thus ΔE can be written as

$$\Delta E = \tfrac{1}{2}(R_{1x}, R_{2x})\begin{pmatrix} \frac{1}{\mathscr{I}_1}+\frac{1}{\mathscr{I}_r} & \frac{1}{\mathscr{I}_r} \\ \frac{1}{\mathscr{I}_r} & \frac{1}{\mathscr{I}_2}+\frac{1}{\mathscr{I}_r}\end{pmatrix}\begin{pmatrix} R_{1x} \\ R_{2x}\end{pmatrix}$$

$$+\tfrac{1}{2}(\mathrm{K}, \mathrm{R}_y)\begin{pmatrix} \dfrac{\mathscr{I}_r}{\mathscr{I}_T(\mathscr{I}_1+\mathscr{I}_2)} & 0 \\ 0 & \dfrac{1}{\mathscr{I}_1}+\dfrac{1}{\mathscr{I}_2} \end{pmatrix}\begin{pmatrix} K \\ R_y \end{pmatrix}$$

$$+\tfrac{1}{2}(R_{1z}, R_{2z})\begin{pmatrix} \dfrac{1}{\mathscr{I}_1}+\dfrac{1}{\mathscr{I}_r} & \dfrac{1}{\mathscr{I}_r} \\ \dfrac{1}{\mathscr{I}_r} & \dfrac{1}{\mathscr{I}_2}+\dfrac{1}{\mathscr{I}_r} \end{pmatrix}\begin{pmatrix} R_{1z} \\ R_{2z} \end{pmatrix} \tag{6}$$

Since the second block is diagonal, we have already found two of the six normal modes. The first corresponds to a tilting of the disintegration axis which produces rigid rotation of the fragments about the symmetry axis. The second mode is a twisting mode in which the fragments bear equal but oppositely directed spins. These modes are exactly the same as those found in the mass-symmetric case. Rather than using K and R_y, it proves convenient (see below) to define the normal coordinates ζ_{TI} and ζ_{TW}, where

$$\zeta_{TI} = K\sqrt{\frac{\mathscr{I}_r}{\mathscr{I}_T(\mathscr{I}_1+\mathscr{I}_2)}}, \tag{7a}$$

$$\zeta_{TW} = R_y\sqrt{\frac{\mathscr{I}_1+\mathscr{I}_2}{\mathscr{I}_1\mathscr{I}_2}}. \tag{7b}$$

For tilting, the fragment spin components of the eigenvector are

$$a_{1TI} = \mathscr{I}_1\sqrt{\frac{\mathscr{I}_T}{\mathscr{I}_r(\mathscr{I}_1+\mathscr{I}_2)}}, \qquad a_{2TI} = \mathscr{I}_2\sqrt{\frac{\mathscr{I}_T}{\mathscr{I}_r(\mathscr{I}_1+\mathscr{I}_2)}}; \tag{8a}$$

for twisting,

$$a_{1TW} = \sqrt{\frac{\mathscr{I}_1\mathscr{I}_2}{\mathscr{I}_1+\mathscr{I}_2}}, \qquad a_{2TW} = -\sqrt{\frac{\mathscr{I}_1\mathscr{I}_2}{\mathscr{I}_1+\mathscr{I}_2}}. \tag{8b}$$

Since the remaining two blocks in eq. (6) are identical, there are two doubly degenerate modes left to be found. The diagonalization process leads to the secular equation

$$\left(\frac{1}{\mathscr{I}_1}+\frac{1}{\mathscr{I}_r}-\lambda\right)\left(\frac{1}{\mathscr{I}_2}+\frac{1}{\mathscr{I}_r}-\lambda\right)-\frac{1}{\mathscr{I}_r^2}=0, \tag{9}$$

which yields the eigenvalues

$$\lambda_\alpha = \frac{1}{2}\left(\frac{1}{\mathscr{I}_1} + \frac{1}{\mathscr{I}_2} + \frac{2}{\mathscr{I}_r} \pm \sqrt{\left(\frac{1}{\mathscr{I}_1} - \frac{1}{\mathscr{I}_2}\right)^2 + \left(\frac{4}{\mathscr{I}_r^2}\right)}\right), \tag{10}$$

where $\alpha = \mathrm{W}$ corresponds to the plus sign and $\alpha = \mathrm{B}$ corresponds to the minus sign. The ratio of the components of the eigenvectors is given by

$$\frac{a_{1\alpha}}{a_{2\alpha}} = \mathscr{I}_r\left(\lambda_\alpha - \frac{1}{\mathscr{I}_2} - \frac{1}{\mathscr{I}_r}\right) = -\frac{\mathscr{I}_r}{2\mathscr{I}^*} \pm \sqrt{1 + \left(\frac{\mathscr{I}_r}{2\mathscr{I}^*}\right)^2}, \tag{11}$$

where $1/\mathscr{I}^* = 1/\mathscr{I}_2 - 1/\mathscr{I}_1$. Note that if the plus sign is taken, the ratio is always positive, indicating that the mode is symmetric. On the other hand, the minus sign corresponds to an antisymmetric mode. The identification of these modes with wriggling-like and bending-like motions is evident. Thus we designate these normal coordinates as $\zeta_{\mathrm{W}x}$, $\zeta_{\mathrm{W}z}$, $\zeta_{\mathrm{B}x}$ and $\zeta_{\mathrm{B}z}$.

The above equation specifies only the ratio of the components of the eigenvectors. The normalization is most conveniently fixed by requiring that the eigenvectors be orthogonal in the vector space in which T is the metric tensor. This requirement leads to

$$a_{1\alpha} = \pm\mathscr{I}_1\left[\frac{\mathscr{I}_2}{\mathscr{I}_1^2\mathscr{I}_r(\mathscr{I}_2+\mathscr{I}_r)\lambda_\alpha^2 + (\mathscr{I}_1+\mathscr{I}_r-2\mathscr{I}_1\mathscr{I}_r\lambda_\alpha)\mathscr{I}_T}\right]^{\frac{1}{2}} \tag{12a}$$

and

$$a_{2\alpha} = \mathscr{I}_2\left[\frac{\mathscr{I}_1}{\mathscr{I}_2^2\mathscr{I}_r(\mathscr{I}_1+\mathscr{I}_r)\lambda_\alpha^2 + (\mathscr{I}_2+\mathscr{I}_r-2\mathscr{I}_2\mathscr{I}_r\lambda_\alpha)\mathscr{I}_T}\right]^{\frac{1}{2}}. \tag{12b}$$

In eq. (12a) the plus sign is to be taken for the wriggling mode whereas the minus sign is to be taken for bending. With this choice of normalization (which is consistent with that used for tilting and twisting), the kinetic energy takes on a very simple form:

$$\Delta E = \tfrac{1}{2}(\zeta_{\mathrm{W}x}^2 + \zeta_{\mathrm{B}x}^2 + \zeta_{\mathrm{T}1}^2 + \zeta_{\mathrm{T}\mathrm{W}}^2 + \zeta_{\mathrm{W}z}^2 + \zeta_{\mathrm{B}z}^2) = \tfrac{1}{2}\sum_\alpha \zeta_\alpha^2. \tag{13}$$

Thus from the point of view of energetics, all the normal modes are placed on an equal footing.

In figs. 2a en b the fragment spin components of the various eigenvectors expressed in units of $\sqrt{\mathscr{I}_0}$, the square root of the moment of inertia of the compound system, are plotted as a function of the mass fraction of fragment one, $U_1 = A_1/A_T$. At symmetry the two fragments carry equal spins for each of the normal modes as expected. Note that the twisting and bending modes have equal spins at symmetry

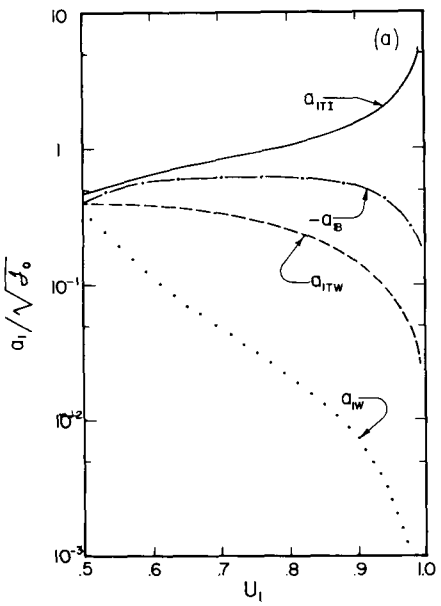

Fig. 2a. The spin components of fragment one for the various normal modes plotted as a function of the mass fraction for fragment one, U_1.

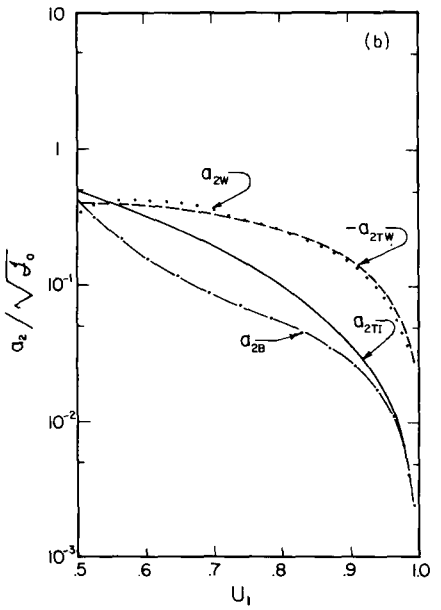

Fig. 2b. The spin components of fragment two as a function of U_1.

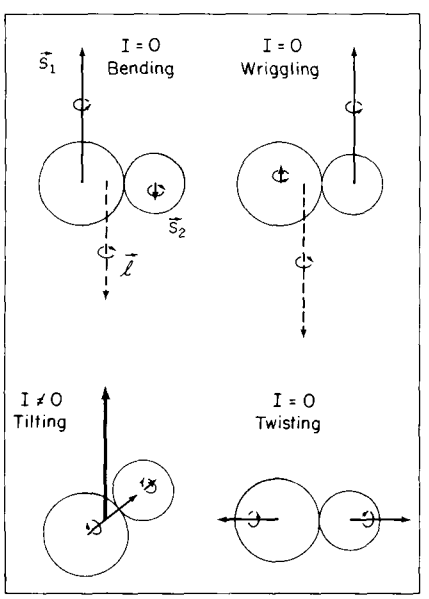

Fig. 3. Schematic illustrating the angular momentum invested in orbital motion and intrinsic fragment spin for each of the normal modes. An asymmetry $U_1 = 0.7$ is assumed.

indicating degeneracies. However, except for twisting the two fragments do not carry equal spins for asymmetric configurations. For the bending-like mode the heavy fragment (fragment one) bears most of the spin. On the other hand, in the case of wriggling the light fragment carries the bulk of the spin. The bending and wriggling modes are complementary in the sense that

$$\frac{a_{1W}}{a_{2W}} = -\frac{a_{2B}}{a_{1B}},$$

as is easily shown using eq. (11). As a further illustration, fig. 3 shows the relative amounts of angular momentum in orbital motion and in intrinsic rotation for the various normal modes. The radii of the fragments correspond to $U_1 = 0.7$ under the assumption that $R \propto U^{1/3}$. For simplicity zero total spin is assumed for all modes except for tilting.

Because of our normalization, the magnitudes of the components of the eigenvectors reflect the fragment spins which result from a fixed energy investment in each of the normal modes. Consequently, the values of the components gives an indication of the importance of the various modes at thermal equilibrium. It is apparent from figs. 2a and b that all of the modes except tilting are suppressed at extreme asymmetries. The suppression of the twisting mode reflects the fact that it is energetically costly to impart spin to the light fragment. On the other hand, the demise of the bending mode results from an increase in the angular momentum associated with the orbital motion which becomes stiffer at large asymmetries ($\mathscr{I}_r \to 0$ as $U \to 1$). Finally, both of these effects contribute to the rapid suppression of the wriggling mode. The tilting mode is exceptional because the heavy fragment bears essentially all of the spin at large asymmetries and because there is no orbital angular momentum associated with it. Now let us turn to the statistical mechanical aspects of the problem.

3. Partition functions and averages

Using the normal modes found in the last section, one can write the classical partition function in the simple form

$$Z \propto \int d\zeta_{Wx} \cdots \int d\zeta_{Bz} \exp\{-(\zeta_{Wx}^2 + \ldots + \zeta_{Bz}^2)/2\tau\} = \prod_\alpha \int d\zeta_\alpha e^{-\zeta_\alpha^2/2\tau} = \prod_\alpha Z_\alpha, \quad (14)$$

where τ is the temperature. For wriggling, bending, and twisting $-\infty \leqq \zeta_\alpha \leqq +\infty$; thus

$$Z_\alpha = \int_{-\infty}^{+\infty} d\zeta_\alpha e^{-\zeta_\alpha^2/2\tau} = \sqrt{2\pi\tau}. \quad (15)$$

The excitation of the tilting mode is limited by the total angular momentum of the

system; i.e. $-I/(a_{1\mathrm{TI}}+a_{2\mathrm{TI}}) \leqq \zeta_{\mathrm{TI}} \leqq I/(a_{1\mathrm{TI}}+a_{2\mathrm{TI}})$. In this case

$$Z_{\mathrm{TI}} = \sqrt{2\pi\tau}\,\mathrm{erf}\left(\frac{I}{\sqrt{2\tau}(a_{1\mathrm{TI}}+a_{2\mathrm{TI}})}\right) = \sqrt{2\pi\tau}\,\mathrm{erf}\left(I\sqrt{\frac{\mathscr{I}_{\mathrm{r}}}{2\tau\mathscr{I}_{\mathrm{T}}(\mathscr{I}_1+\mathscr{I}_2)}}\right). \tag{16}$$

Equipped with these partion functions, it is straightforward to calculate various expectation values. First of all,

$$\langle\zeta_\alpha\rangle = \frac{1}{Z_\alpha}\int \mathrm{d}\zeta_\alpha \zeta_\alpha \mathrm{e}^{-\zeta_\alpha^2/2\tau} = 0 \tag{17}$$

holds for all of the modes. Similarly, it is easy to see that $\langle\zeta_\alpha\zeta_\beta\rangle = 0$ for $\alpha \neq \beta$. This last result is, of course, expected since the normal modes are independent. For bending, wriggling, and twisting,

$$\langle\zeta_\alpha^2\rangle = \frac{1}{Z_\alpha}\int_{-\infty}^{+\infty} \mathrm{d}\zeta_\alpha \zeta_\alpha^2 \mathrm{e}^{-\zeta_\alpha^2/2\tau} = \tau. \tag{18}$$

For tilting,

$$\langle\zeta_{\mathrm{T1}}^2\rangle = \tau\left\{1 - \sqrt{\frac{2}{\pi\tau}}\frac{x\mathrm{e}^{-x^2/2\tau}}{\mathrm{erf}\left(\frac{x}{\sqrt{2\tau}}\right)}\right\}, \tag{19}$$

where

$$x = I/(a_{1\mathrm{TI}}+a_{2\mathrm{TI}}) = I\sqrt{\frac{\mathscr{I}_{\mathrm{r}}}{\mathscr{I}_{\mathrm{T}}(\mathscr{I}_1+\mathscr{I}_2)}}.$$

4. Wriggling and bending

Let us now calculate the various moments of the fragment spin distributions for the wriggling and bending modes. Because of the double degeneracy, the bending and wriggling modes produce angular momenta which are randomly oriented in the xz plane.To be more specific, let us focus our attention on fragment one. The excitation of one of these doubly degenerate modes will produce the spin components R_{1x} and R_{1z}. For the specific case of wriggling,

$$R_{1x} = a_{1\mathrm{W}x}\zeta_{\mathrm{W}x}, \qquad R_{1z} = a_{1\mathrm{W}z}\zeta_{\mathrm{W}z}.$$

If we change to the variables $\zeta^2 = \zeta_{\mathrm{W}x}^2+\zeta_{\mathrm{W}z}^2$ and $\theta = \tan^{-1}(\zeta_{\mathrm{W}x}/\zeta_{\mathrm{W}z})$, the spin of fragment one is

$$S_1 = \sqrt{R_1^2+I_{\mathrm{R}1}^2+2R_1I_{\mathrm{R}1}\cos\theta},$$

where $R_1^2 = R_{1x}^2 + R_{1z}^2$. The partition function is

$$\int_0^\infty d\zeta\zeta \int_0^{2\pi} d\theta e^{-\zeta^2/2\tau} = 2\pi\tau.$$

Thus the average spin of fragment one is

$$\langle S_1 \rangle = \frac{1}{2\pi\tau} \int_0^\infty d\zeta\zeta e^{-\zeta^2/2\tau} \int_0^{2\pi} d\theta \sqrt{R_1^2 + I_{R1}^2 + 2R_1 I_{R1} \cos\theta}.$$

As has been shown previously [11]), the integral over θ in the above equation can be accurately approximated by $I_{R1} + R_1^2/4I_{R1}$ for $R_1 < I_{R1}$ and by $R_1 + I_{R1}^2/4R_1$ for $R_1 > I_{R1}$. Thus

$$\langle S_1 \rangle \approx \frac{1}{\tau} \int_0^{I_{R1}/a_{1W}} d\zeta\zeta e^{-\zeta^2/2\tau} (I_{R1} + R_1^2/4I_{R1}) + \frac{1}{\tau} \int_{I_{R1}/a_{1W}}^\infty d\zeta\zeta e^{-\zeta^2/2\tau} (R_1 + I_{R1}^2/4R_1)$$

$$= I_{R1} + \frac{a_{1W}^2 \tau}{2I_{R1}} - \frac{1}{2}\left(\frac{a_{1W}^2 \tau}{I_{R1}} + \frac{I_{R1}}{2}\right) \exp\left(-\frac{I_{R1}^2}{2a_{1W}^2 \tau}\right)$$

$$+ \sqrt{2\pi\tau}\left(\frac{a_{1W}}{2} + \frac{I_{R1}^2}{8\tau a_{1W}}\right) \operatorname{erfc}\left(\frac{I_{R1}}{a_{1W}\sqrt{2\tau}}\right). \tag{20}$$

At symmetry $a_{1W}^2 = \mathscr{I}_r \mathscr{I}_1 / 2(\mathscr{I}_r + 2\mathscr{I}_1)$. Substitution of this expression into eq. (20) yields the same value of $\langle S_1 \rangle$ obtained for the symmetric case [11]). In the limit of large I_{R1}, eq. (20) yields

$$\langle S_1 \rangle \approx I_{R1} + \frac{a_{1W}^2 \tau}{2I_{R1}}. \tag{21}$$

The calculation of $\langle S_1^2 \rangle$ is somewhat easier:

$$\langle S_1^2 \rangle = \langle R_1^2 + I_{R1}^2 + 2R_1 I_{R1} \cos\theta \rangle$$

$$= \frac{1}{2\pi\tau} \int_0^\infty d\zeta\zeta \int_0^{2\pi} d\theta (R_1^2 + I_{R1}^2 + 2R_1 I_{R1} \cos\theta) e^{-\zeta^2/2\tau}$$

$$= I_{R1}^2 + 2\tau a_{1W}^2, \tag{22}$$

Using eqs. (20) and (22) one can readily calculate the sigma of the spin distribution for fragment one, σ_{1W}. For large I_{R1},

$$\sigma_{1W}^2 \approx a_{1W}^2 \tau. \tag{23}$$

For measurements which are not sensitive the spin distributions of the individual fragments (e.g. γ-ray multiplicity experiments), it is more appropriate to consider

the total fragement spin S_T. The quantity $\langle S_T \rangle = \langle |S_1| \rangle + \langle |S_2| \rangle$ is obviously easy to calculate using eq. (20). However, the calculation of σ_W is a bit mor involved because

$$\begin{aligned}\sigma_W^2 &= \langle (|S_1| + |S_2|)^2 \rangle - \langle |S_1| + |S_2| \rangle^2 \\ &= \sigma_{1W}^2 + \sigma_{2W}^2 + 2\mathrm{cov}(S_1, S_2) \\ &= \sigma_{1W}^2 + \sigma_{2W}^2 + 2(\langle S_1 S_2 \rangle - \langle S_1 \rangle \langle S_2 \rangle).\end{aligned} \tag{24}$$

It is not so simple to evaluate the covariance terms with the same approximation technique utilized in deriving eq. (20). Hence let us make the more extreme approximation that I_{R1} and I_{R2} are large compared to R_1 and R_2, respectively. In this case one can use eq. (21) to obtain the result

$$\langle S_1 \rangle \langle S_2 \rangle \approx \left(I_{R1} + \frac{a_{1W}^2 \tau}{2 I_{R1}} \right) \left(I_{R2} + \frac{a_{2W}^2 \tau}{2 I_{R2}} \right). \tag{25}$$

To second order in R/I_R,

$$\langle S_1 S_2 \rangle \approx I_{R1} I_{R2} + \frac{1}{2} \frac{I_{R2}}{I_{R1}} a_{1W}^2 \tau + \frac{1}{2} \frac{I_{R1}}{I_{R2}} a_{2W}^2 \tau + a_{1W} a_{2W} \tau. \tag{26}$$

Combining eqs. (25) and (26) one obtains

$$\mathrm{cov}(S_1, S_2) = a_{1W} a_{2W} \tau - \frac{a_{1W}^2 a_{2W}^2 \tau^2}{4 I_{R1} I_{R2}} \approx a_{1W} a_{2W} \tau. \tag{27}$$

At first glance it might appear that the usefulness of the above equation is very limited because of the restriction $R < I_R$. This condition is obviously not satisfied at large asymmetries because $I_R \to 0$ for the light fragment. However, as the asymmetry increases, the importance of the covariance term diminishes, and, although the assumption $R < I_R$ is not justified, eq. (27) can still be used without introducing any appreciable error.

If one also uses the expression for σ_{1W} and σ_{2W} for $I_R > R$, one obtains the very simple result

$$\sigma_W^2 \approx (a_{1W} + a_{2W})^2 \tau. \tag{28}$$

At symmetry this equation yields

$$\sigma_W^2 = 4 a_{1W}^2 \tau = \frac{2 \mathscr{I}_1 \mathscr{I}_r}{\mathscr{I}_r + 2 \mathscr{I}_1} \tau,$$

as obtained previously [11]).

In the preceeding paragraphs the discussion has concentrated on the wriggling modes. The treatment of the degenerate bending modes is formally identical. The only modifications that need to be made are the replacement of a_{1W} with $|a_{1B}|$ and a_{2W} with a_{2B}.

5. Tilting and twisting modes

For the tilting mode the spin of fragment one is

$$S_1 = \left[\left(\frac{\mathscr{I}_1}{\mathscr{I}_T}\right)^2 (I^2 - K^2) + \frac{\mathscr{I}_1^2 K^2}{(\mathscr{I}_1 + \mathscr{I}_2)^2}\right]^{\frac{1}{2}}$$

$$= I_{R1}\left[1 + \frac{1}{I_{R1}^2}\left(a_{1TI}^2 - \left(\frac{\mathscr{I}_1}{\mathscr{I}_T}\right)^2 (a_{1TI} + a_{2TI})^2\right)\zeta_{TI}^2\right]^{\frac{1}{2}}.$$

To second order

$$\langle S_1\rangle \approx I_{R1} + \frac{1}{2I_{R1}}\left(a_{1TI}^2 - \left(\frac{\mathscr{I}_1}{\mathscr{I}_T}\right)^2 (a_{1TI} + a_{2TI})^2\right)\langle\zeta_{TI}^2\rangle, \tag{29}$$

where $\langle\zeta_{T1}^2\rangle$ can be obtained from eq. (19). For large I_{R1}, $\langle\zeta_{TI}^2\rangle \approx \tau$. In this limit

$$\langle S_1\rangle \approx I_{R1} + \frac{\mathscr{I}_1^2(\mathscr{I}_r + 2(\mathscr{I}_1 + \mathscr{I}_2))}{2I_{R1}\mathscr{I}_T(\mathscr{I}_1 + \mathscr{I}_2)}\tau, \tag{30}$$

where we have used the expression in eqs. (8a). Averaging the square of S_1, one obtains

$$\langle S_1^2\rangle = I_{R1}^2 + \left(a_{1TI}^2 - \left(\frac{\mathscr{I}_1}{\mathscr{I}_T}\right)^2 (a_{1TI} + a_{2TI})^2\right)\langle\zeta_{TI}^2\rangle$$

$$\approx I_{R1}^2 + \frac{\mathscr{I}_1^2(\mathscr{I}_r + 2(\mathscr{I}_1 + \mathscr{I}_2))}{\mathscr{I}_T(\mathscr{I}_1 + \mathscr{I}_2)}\tau, \tag{31}$$

where the approximate form corresponds to the high-spin limit. As noted for the symmetric case, the fluctuations in the spin produced by tilting are small. In fact, $\sigma_T^2 = 0$ to second order.

Lastly, let us consider the twisting mode. For fragment one

$$\langle S_1\rangle = \frac{1}{\sqrt{2\pi\tau}}\int_{-\infty}^{+\infty} d\zeta_{TW}[I_{R1}^2 + a_{1TW}^2\zeta_{TW}^2]^{\frac{1}{2}} e^{-\zeta_{TW}^2/2\tau}. \tag{32}$$

A good approximation to this integral can be obtained by expanding the radical in powers of a_{1TW}/I_{R1} for $\zeta_{TW} < I_{R1}/a_{1TW}$ and in powers of I_{R1}/a_{1TW} for $\zeta_{TW} > I_{R1}/a_{1TW}$. Some care must be taken in this procedure. To second order,

$$\langle S_1\rangle \approx \left(I_{R1} + \frac{a_{1TW}^2\tau}{2I_{R1}}\right)\mathrm{erf}\left(\frac{I_{R1}}{a_{1TW}\sqrt{2\tau}}\right) + \frac{a_{1TW}}{2}\sqrt{\frac{2\tau}{\pi}}\, e^{-I_{R1}^2/2a_{1TW}^2\tau}$$

$$+ \frac{I_{R1}^2}{2a_{1TW}\sqrt{2\pi\tau}} E_1\left(\frac{I_{R1}^2}{2a_{1TW}^2\tau}\right), \tag{33}$$

where $E_1(x)$ is the exponential integral

$$E_1(x) = \int_x^\infty \mathrm{d}t^{-1}\mathrm{e}^{-t}.$$

In the limit of small I_{R1},

$$\langle S_1 \rangle \approx a_{1TW}\sqrt{\frac{2\tau}{\pi}} = \sqrt{\frac{2\tau \mathscr{I}_1 \mathscr{I}_2}{\pi(\mathscr{I}_1 + \mathscr{I}_2)}}\,; \tag{34}$$

whereas for large I_{R1},

$$\begin{aligned}\langle S_1 \rangle &\approx I_{R1} + \frac{a_{1TW}^2 \tau}{2I_{R1}} \\ &= I_{R1} + \frac{\mathscr{I}_1 \mathscr{I}_2}{2I_{R1}(\mathscr{I}_1 + \mathscr{I}_2)}\tau.\end{aligned} \tag{35}$$

One can readily show that

$$\begin{aligned}\langle S_1^2 \rangle &= I_{R1}^2 + a_{1TW}^2 \tau \\ &= I_{R1}^2 + \frac{\mathscr{I}_1 \mathscr{I}_2}{\mathscr{I}_1 + \mathscr{I}_2}\tau.\end{aligned} \tag{36}$$

The sigma of the spin distribution for fragment one can be obtained from eqs. (33) and (36). For large spin $\sigma_{1TW}^2 \simeq 0$, while for small I_{R1},

$$\sigma_{1TW}^2 \approx a_{1TW}^2 \tau \left(1 - \frac{2}{\pi}\right). \tag{37}$$

Near symmetry the fluctuation in the total spin distribution due to twisting, σ_{TW}, is small. For fairly asymmetric mass splits $\sigma_{TW}^2 \approx \sigma_{2TW}^2$, where we have assumed that fragment two is the light fragment. Thus the spreading in the spin distribution due to twisting is generally small.

6. Some examples

The model described in the preceeding sections can be applied to a number of aspects of heavy-ion collisions. As examples, we shall consider the effects of the collective modes on the spin distribution of the fragments and on the angular distributions of sequential fission fragments for a typical heavy-ion reaction. We have chosen the reaction ^{197}Au + 600 MeV ^{86}Kr because it is a well-studied case [2,12]) and because it was also used in the comparison with the symmetric sphere model [11]).

The average orbital angular momentum in the ^{197}Au + ^{86}Kr system is about 190$\hbar$. The corresponding temperature for this l-wave is estimated to be 1.78 MeV. In the interest of simplicity, we shall assume that both of these quantities are independent of asymmetry. In reality, the angular momentum is expected to be fractionated

along the mass asymmetry coordinate even at equilibrium [11,12]). The temperature will also vary with asymmetry.

The first point to be considered is the correction to the fragment spins due to the statistical excitation of collective modes. Using eqs. (8) and (12) the spin components of the various normal modes are readily calculated. The spins arising from wriggling, bending, tilting and twisting are then calculated using eqs. (20), (29) and (33). The sum of the fragment spins divided by the total spin arising from rigid rotation is plotted in fig. 4. Even for this rather high l-wave, the correction to the fragment spins approaches 20 % for nearly symmetric exit channels. However, as the asymmetry increases, the correction decreases rather rapidly (note that the entrance channel corresponds to $U_1 = 0.7$). This trend is easily understood; the excitation of the various collective modes is suppressed at large asymmetries as discussed earlier.

We have also calculated the sigmas of the spin distributions of the fragments arising from the wriggling and the bending modes using eq. (28). In fig. 5 the ratio of these quantities to the total fragment spin is plotted as a function of the mass asymmetry. The ratio $\sigma_T/\langle S_T \rangle$ is also given (tilting and twisting have been neglected in σ_T since these modes yield relatively small contributions). Once again one observes that the influence of the collective modes is strongest near symmetry. In this region the dispersion is $> 30\,\%$. As the asymmetry is increased, however, the relative width of the spin distribution decreases. This effect is particularly strong for the wriggling mode because the light fragment bears most of the spin (see figs. 2a and b).

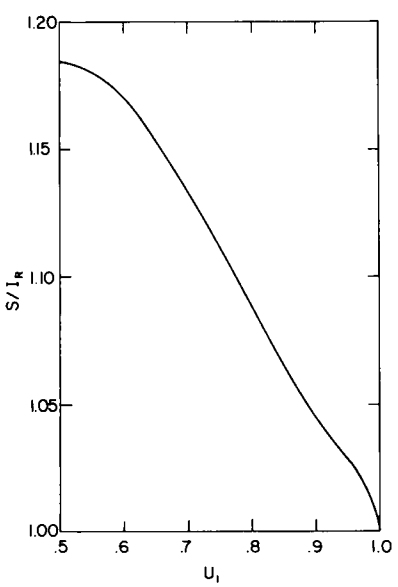

Fig. 4. The ratio of the average total fragment spin to the spin arising from rigid rotation as a function of the mass fraction for fragment one for the $^{197}Au+^{86}Kr$ reaction (see text).

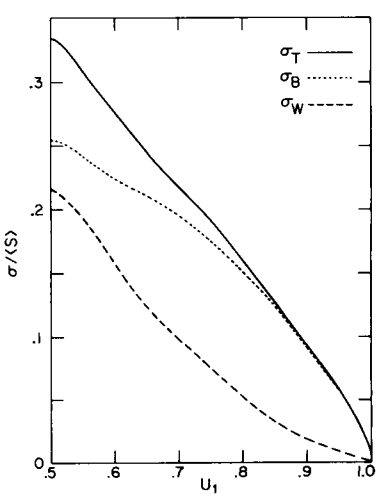

Fig. 5. The ratio of the sigma of the spin distribution to the average spin for wriggling, bending, and wriggling plus bending as a function of the U_1 for the $^{197}Au+^{86}Kr$ reaction (see text).

The effect is less pronounced for bending since the heavy fragment carries most of the angular momentum.

The large dispersion in the spin distributions of the fragments can partially explain the large widths observed in γ-ray multiplicity distributions [13]). However, extreme caution should be exercised since the excitation of collective modes is certainly not the only source of dispersion. The contribution from the width of the orbital angular-momentum distribution must also be properly included taking angular momentum fractionation effects into account [11,12]).

As a final example we shall consider the effect of the various collective modes on the spin alignment in deep-inelastic reactions. Since the problem of the angular distributions of light particles, fission fragments, and γ-rays has recently been dealt with quite extensively [14,15]), we shall confine ourselves to a simple and schematic example which illustrates the application of the current model. In particular, let us consider the in-plane and out-of-plane angular distributions of sequential fission fragments from the ^{197}Au+^{86}Kr reaction for $l = 190\hbar$.

If the distribution governing the orientation of the spin of the fissioning nucleus (fragment one) is of the form

$$P(\boldsymbol{I}) \propto \exp\left[-\frac{I_x^2}{2\sigma_x^2} - \frac{I_y^2}{2\sigma_y^2} - \frac{(I_z - \langle I_z\rangle)^2}{2\sigma_z^2}\right], \tag{38}$$

the angular distribution of the fission fragments is given by [8])

$$W(\theta,\phi) \propto \frac{1}{S(\theta,\phi)} \exp\{-\tfrac{1}{2}[I_z\cos\theta/S(\theta,\phi)]^2\}, \tag{39}$$

where

$$S^2(\theta,\phi) = K_0^2 + (\sigma_x^2\cos^2\phi + \sigma_y^2\sin^2\phi)\sin^2\theta + \sigma_z^2\cos^2\theta. \tag{40}$$

The sigmas in the above equations are given by

$$\sigma_x^2 = \sigma_z^2 = a_{\mathrm{B}}^2\langle\zeta_{\mathrm{B}}^2\rangle + a_{\mathrm{W}}^2\langle\zeta_{\mathrm{W}}^2\rangle = \frac{\mathscr{I}_1(\mathscr{I}_2+\mathscr{I}_{\mathrm{r}})}{\mathscr{I}_{\mathrm{T}}}\tau, \tag{41a}$$

$$\sigma_y^2 = a_{\mathrm{TI}}^2\langle\zeta_{\mathrm{TI}}^2\rangle + a_{\mathrm{TW}}^2\langle\zeta_{\mathrm{TW}}^2\rangle \approx \frac{\mathscr{I}_1(\mathscr{I}_1+\mathscr{I}_{\mathrm{r}})}{\mathscr{I}_{\mathrm{r}}}\tau. \tag{41b}$$

The approximate form given in eq. (41b) corresponds to the high-spin limit in which $\langle\zeta_{\mathrm{T}}^2\rangle \approx \tau$.In other situations, eq. (19) must be used for $\langle\zeta_{\mathrm{TI}}^2\rangle$.

Using eq. (41) we find $\sigma_x = \sigma_z = 13\hbar$ and $\sigma_y = 18\hbar$ for the entrance channel asymmetry ($U = 0.7$). Assuming $K_0 = 10\hbar$ and $I_z = 54\hbar$ one obtains the in-plane and out-of-plane distributions shown in fig. 6 (see solid curves). The out-of-plane distributions are strongly anisotropic as observed experimentally. Interestingly enough there is also a weak in-plane anisotropy; a shallow minimum occurs along the line of centers. The angular distributions are rather sensitive to the exit-channel

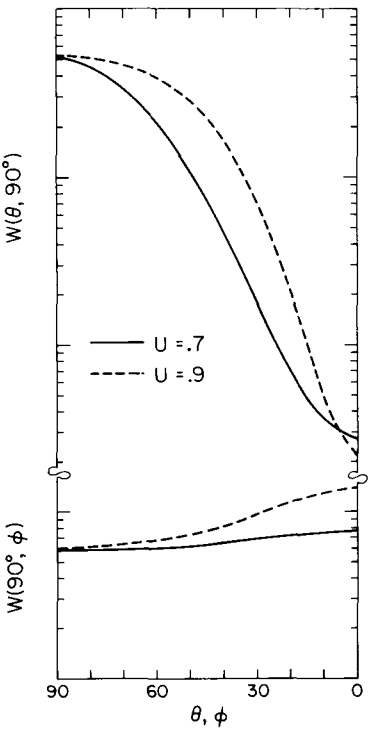

Fig. 6. Calculated out-of-plane and in-plane angular distributions of sequential fission fragments for the ^{197}Au+600 MeV ^{86}Kr reaction for $U = 0.7$ (the entrance channel) and $U = 0.9$. Note that the line of centers is situated at $\theta = 90°$ and $\phi = 90°$.

asymmetry. As an illustration we have performed a similar calculation for $U = 0.9$ (see dashed curves in fig. 6). For this larger asymmetry, the out-of-plane distribution broadens due to the increased tilting of the decay axis of the projectile and target nuclei. At the same time, the predominant spin fluctuations about the decay axis give rise to an appreciable in-plane anisotropy.

At the current time, the experimental situation regarding the in-plane angular distributions is unclear. Measurements on the systems ^{58}Ni and ^{90}Zr+^{208}Pb and ^{238}U indicate essentially isotropic distributions [4]). On the other hand, studies of the reaction ^{209}Bi+^{86}Kr, ^{197}Au+^{20}Ne, and ^{238}U+^{20}Ne do show in-plane anisotropies with a maximum along the expected recoil direction of the target-like fragment [3, 16]). In these cases, the anisotropies become more pronounced as the exit-channel asymmetry increases in qualitative agreement with the present model. However, the quantitative comparison of the experimental data with the model prediction is not straightforward. In the model, the relevant direction is that of the line of centers at the time of scission when the interaction between the fragments ceases and the instantaneous partition of the total angular momentum is fixed in the system. Because this direction generally does not coincide with the recoil direction or any other

experimentally determined direction, it is difficult to pass judgement on the statistical model at this time.

7. Summary

In conclusion, we have described a simple, two-sphere model for the statistical excitation of various collective modes in heavy-ion reactions. It has been found that the angular momentum carried by these modes is strongly dependent on the mass asymmetry of the system. In particular, all of the modes except tilting tend to be suppressed at large asymmetries. Analytic expressions for the first and second moments of the spin distributions of the fragments have been presented. In addition, the effect of the excitation of these modes on the spin alignment has been explored.

This work was supported by the US Department of Energy under contract DE-AS05-80ER01565.

References

1) M. Berlanger, M. A. Deleplanque, C. Gerschel, F. Hanappe, M. Leblanc, J. F. Mayault, C. Ngô, D. Paya, N. Perrin, J. Peter, B. Tamain and L. Valentin, J. Phys. Lett. **L37** (1976) 323
2) G. J. Wozniak, R. P. Schmitt, P. Glässel, R. C. Jared, G. Bizard and L. G. Moretto, Phys. Rev. Lett. **40** (1978) 1436
3) P. Dyer, R. J. Puigh, R. Vandenbosch, T. D. Thomas and M. S. Zisman, Phys. Rev. Lett. **39** (1977) 392
4) H. v. Harrach, P. Glässel, Y. Civelekoglu, R. Manner and H. J. Specht, Phys. Rev. Lett. **42** (1979) 1728
5) R. A. Dayras, R. G. Stokstad, C. B. Fulmer, D. C. Hensley, M. L. Halbert, R. L. Robinson, A. H. Snell, D. G. Sarantites, L. Westerberg and J. H. Barker, Phys. Rev. Lett. **42** (1979) 697
6) P. Aguer, R. P. Schmitt, G. J. Wozniak, D. Habs, R. M. Diamond, C. Ellegaard, D. L. Hillis, C. C. Hsu, G. J. Mathews, L. G. Moretto, G. U. Rattazzi, C. P. Roulet and F. S. Stephens, Phys. Rev. Lett. **43** (1979) 1778
7) G. J. Wozniak, R. J. McDonald, A. J. Pacheco, C. C. Hsu, D. J. Morrissey, L. G. Sobotka, L. G. Moretto, S. Shih, C. Schück, R. M. Diamond, H. Kluge and F. S. Stephens, Phys. Rev. Lett. **45** (1980) 1081
8) R. A. Broglia, G. Pollarolo, C. H. Dasso and T. Døssing, Phys. Rev. Lett. **43** (1979) 1649
9) S. Ayik, G. Wolschin and W. Nörenberg, Z. Phys. **A286** (1978) 271
10) R. Vandenbosch, Phys. Rev. **C20** (1979) 171
11) L. G. Moretto and R. P. Schmitt, Phys. Rev. **C21** (1980) 204
12) M. M. Aleonard, G. J. Wozniak, P. Glässel, M. A. Deleplanque, R. M. Diamond, L. G. Moretto, R. P. Schmitt and F. S. Stephens, Phys. Rev. Lett. **40** (1978) 622
13) P. R. Christensen, F. Folkmann, O. Hansen, O. Nathan, N. Trautner, F. Videbæk, S. Y. van der Werf, H. C. Britt, R. P. Chestnut, H. Freiesleben and F. Pühlhofer, Phys. Rev. Lett. **40** (1978) 1245
14) T. Døssing, Nucl. Phys. **A357** (1981) 488
15) L. G. Moretto, S. K. Blau and A. J. Pacheco, Nucl. Phys. **A364** (1981) 125
16) D. J. Morrissey, G. J. Wozniak, L. G. Sobotka, A. J. Pacheco, C. C. Hsu, R. J. McDonald and L. G. Moretto, Lawrence Berkeley Laboratory report LBL-12181, to be published